References and Notes

1. C. R. Jones *et al.*, *Nature Med.* **5**, 1062 (1999).
2. J. C. Dunlap, *Cell* **96**, 271 (1999).
3. D. R. Weaver, *J. Biol. Rhythms* **13**, 100 (1998).
4. S. M. Reppert, *Neuron* **21**, 1 (1998).
5. D. P. King and J. S. Takahashi, *Annu. Rev. Neurosci.* **23**, 713 (2000).
6. M. J. Hamblen-Coyle *et al.*, *J. Insect Behav.* **5**, 417 (1992).
7. K. Wager-Smith, S. A. Kay, *Nature Genet.*, **26**, 23 (2000).
8. L. P. Shearman *et al.*, *Science* **288**, 1013 (2000).
9. Individuals who did not meet either the conservative affected or unaffected criteria were classified as unknown. Venous blood samples were gathered from individuals from ASPS families who were likely to contribute to linkage information. Participants signed a "Consent of Participation" form, which was approved by the Institutional Review Board for Human Research at the University of Utah School of Medicine. High–molecular weight genomic DNA was isolated from whole-blood lysates, and lymphoblastoid cell lines were transformed with Epstein-Barr virus, as described (*36*).
10. The fluorescently labeled markers were used to amplify genomic DNA in total reaction volumes of 20 μl in a MJR PTC-200 thermocycler (MJ Research, Watertown, MA). The products were visualized on an Applied Biosystems model 377 and analyzed by the Genotyper peak-calling software. Pairwise two-point linkage analysis with MLINK of the LINKAGE program was used. Disease penetrance was set at 0.95, without a gender difference, and the normal and FASPS allele frequencies were set at 0.999 and 0.001, respectively.
11. Manual genotyping was carried out after PCR of DNA samples with appropriate primers, as previously described (*36*).
12. K. L. Toh *et al.*, data not shown.
13. Markers D2S338, D2S2338, D2S2285, D2S2253, D2S125, D2S395, D2S140, D2S2986, and D2S2987 (from centromere to telomere) were used for genotyping and haplotype analysis.
14. C. Dib *et al.*, *Nature* **380**, 152 (1996).
15. U. Albrecht *et al.*, *Cell* **91**, 1055 (1997).
16. R. J. Konopka, S. Benzer, *Proc. Natl. Acad. Sci. U.S.A.* **68**, 2112 (1971).
17. B. Zheng *et al.*, *Nature* **400**, 169 (1999).
18. E. B. Klerman *et al.*, *Am. J. Physiol.* **270**, R271 (1996).
19. J. Duffy *et al.*, Sleep **22**, S92 (1999).
20. M. J. Zylka *et al.*, *Neuron* **20**, 1103 (1998).
21. Human lymphoblast cultures were treated with cholcimid (0.025 mg/ml) at 37°C for 1.5 hours. Coloemid treated cultures were pelleted at 500*g* at room temperature for 8 min. Pellets were then resuspended with 0.075M KCl (3 ml per pellet) for 15 min at room temperature. Cells were then fixed in 3:1 MeOH: acetic acid and stored at 4°C. Human bacterial artificial chromosomes (BACs) were labeled with spectrum orange using a nick translation kit per the manufacturers protocol (Vysis, Downers Grove, IL). Slides were prepared by dropping fixed cells onto glass slides and washing with excess fixative. The slides were then washed in acetic acid for 35 min at room temperature and were dehydrated for 2 min each in 70, 85, and finally 100% EtOH. Chromosomes were denatured in 70% formamide in 2×SSC at 74°C for 5 min, and slides were dehydrated again as above except in ice-cold EtOH. Two micrograms of labeled probe was blocked with 2 μg of human Cot-1 DNA in Hybrisol VI (ONCOR, Gaithersburg, MD). The probe mixture was denatured at 74°C for 5 min and then pre-annealed at 37°C for 15 min. Twelve microliters of pre-annealed probe was applied per slide, a cover slip was added, and edges were sealed with rubber cement. Slides were hybridized in a darkened, humidified chamber for 16 hours at 37°C. Hybridized slides were then washed in 0.4× SSC containing 0.1% Tween-20 at 74°C for 2 min, and then 1 min at room temperature in 2× standard saline citrate (SSC). Slides were allowed to dry in the dark at room temperature and were stained with 4′,6′-diamidino-2-phenylindole (DAPI) (Vector labs, Burlingame, CA) for chromosome visualization.
22. The h*Per2* intron-exon boundaries were determined in order to carry out the mutational analysis. Intron-exon boundaries of the h*Per2* gene were obtained by a combination of direct sequencing of h*Per2* BAC DNA and sequencing of PCR products from genomic DNA with primers distributed along the entire cDNA. Intronic sequence of at least 100 base pairs flanking each exon boundary was obtained. Intron sizes were determined directly from genomic sequence or estimated by the size of PCR products amplified using oligonucleotides from adjacent exons. All sequencing reactions were carried out with an Applied BioSystems model 377 DNA sequencer (Foster City, CA).
23. SSCP was carried out as described (*36*). PCR products were diluted, denatured, and electrophoresed through acrylamide gels and visualized on x-ray film at −80°C for 12 to 24 hours. Aberrant SSCP bands were cut directly from the dried gels and sequenced as described (*36*).
24. Complementary DNA clones encoding m*Per2* and h*Per2* were PCR amplified from the corresponding plasmids and cloned into the pCS2 + MT (myc-epitope tagged) vector as previously described (*25*). Site-directed mutagenesis of the serine residue at position 662 of hPER2 and the homologous serine (659) of mPER2 were performed to substitute a glycine residue. Mutagenesis was carried out with the QuikChange Site-directed Mutagenesis Kit (Stratagene) using the protocol outlined therein. Eco RI–Xba I fragments encoding amino acids 474 to 815 of hPER2 (and the corresponding amino acids 472 to 804 of mPER2) were PCR-amplified with primers containing Eco RI and Xba I sites, gel-purified with the GENECLEAN kit (BIO 101, Vista, CA) and were directionally cloned into the Eco RI–Xba I sites of the pCS2 + MT vector. Expression from an SP6 promoter generates 6-myc-tagged peptides. A series of 3′ deletion mutations of m*Per2* were constructed (encoding amino acids 1 to 554, 1 to 763, 1 to 810, and 1 to 904) for use in mapping the binding site for CKIε, as previously described for m*Per1* (*25*). All constructs were confirmed by sequencing.
25. E. Vielhaber *et al.*, *Mol. Cell. Biol.* **20**, 4888 (2000).
26. B. Kloss *et al.*, *Cell* **94**, 97 (1998).
27. P. L. Lowrey *et al.*, *Science* **288**, 483 (2000).
28. Transcription and translation of h*Per2* and m*Per2* inserts were performed in vitro in the presence of ^{35}S-methionine with the TnT SP6 Coupled Reticulocyte Lysate System (Promega) over a period of 90 min at 30°C. The labeled products were incubated with CKIε in buffer containing phosphatase inhibitors [25 mM Tris.HCl, pH 7.5, 15% glycerol, 20 mM NaF, 170 nM okadaic acid, 2 mM dithiotreitol (DTT), 10 mM β-glycerol phosphate, and 150 μM ATP]. Twenty-microliter aliquots were removed at selected time points and boiled with SDS gel-loading buffer (0.1% bromophenol blue, 50 mM Tris HCl, pH 6.8, 0.1 M DTT, 2% SDS, 10% glycerol) to stop the reaction. At the end of the experiment, 20-μl aliquots were digested with 35 units of calf intestinal phosphatase in buffer (50 mM Tris HCl, pH 7.9, 10 mM $MgCl_2$, 0.1M NaCl, 1 mM DTT) for 30 min where indicated. All products were analyzed by electrophoresis in 8% SDS–polyacrylamide gels (SDS-PAGE) with an acrylamide:bis-acrylamide ratio of 120:1 to enhance mobility shifts. The gels were fixed and dried and the bands visualized using PhosphorImager screens scanned with Scanner Control SI software (Molecular Dynamics, Sunnyvale, CA).
29. H. Flotow *et al.*, *J. Biol. Chem.* **265**, 14264 (1990).
30. A. Cegielska *et al.*, *J. Virol.* **68**, 269 (1994).
31. N. Dumaz, D. M. Milne, D. W. Meek, *FEBS Lett.* **463**, 312 (1999).
32. K. Sakaguchi *et al.*, *J. Biol. Chem.* **275**, 9278 (2000).
33. J. L. Price *et al.*, *Cell* **94**, 83 (1998).
34. G. A. Keesler *et al.*, *Neuroreport* **11**, 951 (2000).
35. Web text is available at *Science* Online at www.sciencemag.org/cgi/content/full/1057499/DC1.
36. L. J. Ptacek *et al.*, *Cell* **77**, 863 (1994).
37. Single-letter abbreviations for the amino acid residues are as follows: A, Ala; C, Cys; D, Asp; E, Glu; F, Phe; G, Gly; H, His; I, Ile; K, Lys; L, Leu; M, Met; N, Asn; P, Pro; Q, Gln; R, Arg; S, Ser; T, Thr; V, Val; W, Trp; and Y, Tyr.

38. We thank the families who participated in this work, A. Meloni-Ehrig and F. Orfino for technical help, and to G. A. Keesler, E. Vielhaber, and V. Hill for helpful discussions and reagents. Supported by NIH grants HL/HD 59596 (L.J.P.), CA71074 (D.M.V.), and Public Health Service research grant M01-RR00064 from the National Center for Research Resources. L. J. P. is an Investigator of the Howard Hughes Medical Institute.

15 November 2000; accepted 18 December 2000
Published online 11 January 2001;
10.1126/science.1057499
Include this information when citing this paper.

TRP-PLIK, a Bifunctional Protein with Kinase and Ion Channel Activities

Loren W. Runnels, Lixia Yue, David E. Clapham*

We cloned and characterized a protein kinase and ion channel, TRP-PLIK. As part of the long transient receptor potential channel subfamily implicated in control of cell division, it is a protein that is both an ion channel and a protein kinase. TRP-PLIK phosphorylated itself, displayed a wide tissue distribution, and, when expressed in CHO-K1 cells, constituted a nonselective, calcium-permeant, 105-picosiemen, steeply outwardly rectifying conductance. The zinc finger containing α-kinase domain was functional. Inactivation of the kinase activity by site-directed mutagenesis and the channel's dependence on intracellular adenosine triphosphate (ATP) demonstrated that the channel's kinase activity is essential for channel function.

Phototransduction in *Drosophila* invokes phospholipase C (PLC)–mediated activation of transient receptor potential (TRP) channels, leading to membrane depolarization (*1*, *2*). The mammalian TRP channel family may be divided by sequence similarity into short, long, and osm 9–like subfamilies [reviewed in (*3*)]. Receptor-mediated stimulation of PLC activates many members of the short TRP channels, and physical or chemical stimuli activate isoforms of the osm 9–like TRP channel. Long TRP channels (LTRPC), such

as melastatin, MTR1, and TRP-PLIK, are distinguished by their long coding sequences. Melastatin expression correlates with melanocytic tumor progression, whereas MTR1 is associated with Beckwith-Wiedemann syndrome and a predisposition to neoplasias (*3*). The gating mechanisms of the LTRPC group are unknown.

A yeast two-hybrid (Y2H) screen of a rat brain library with the C2 domain–containing COOH-terminus of PLC-β_1 as bait identified a potential interacting partner with similarity to *Dictyostelium* myosin heavy chain kinase B (MHCK B) and eukaryotic elongation factor 2 kinase (eEF-2 kinase). Rapid amplification of cDNA ends (RACE) experiments based on the rat Y2H clones revealed one open reading frame encoding a putative kinase with 347 amino acids and a predicted molecular mass of 39.6 kD (*4*). A BLAST search with the sequence of the Y2H clone against the NCBI nonredundant nucleotide database revealed that the sequence is part of a larger open reading frame within a 7105–base pair (bp) transcript (accession number: AF149013; ChaK) encoding an 1863–amino acid protein with a predicted molecular mass of 212.4 kD (Fig. 1A). We cloned the predicted larger protein directly by polymerase chain reaction (PCR) from mouse brain cDNA (*5*). Comparison of the deduced amino acid sequence with those in the nucleotide and protein databanks demonstrated substantial similarity of ChaK to TRP family members, with greatest similarity to a member of the LTRPC group, melastatin. We designated the smaller protein PLIK, for "phospholipase C interacting kinase," and the larger protein TRP-PLIK. The interaction of PLIK with PLC-β_1 was confirmed by coimmunoprecipitation of expressed proteins in CHO-K1 cells and by glutathione S-transferase (GST) pull-down purification (*6*).

Howard Hughes Medical Institute, Department of Cardiology, Department of Neurobiology, Harvard Medical School, 1309 Enders Building, 320 Longwood Avenue, Children's Hospital, Boston, MA 02115, USA.
*To whom correspondence should be addressed. E-mail: clapham@rascal.med.harvard.edu

Northern blot analysis of polyadenylated RNAs revealed an ~8-kb transcript in brain and skeletal muscle, with stronger signals in kidney, heart, liver, and spleen, consistent with the 7105-bp transcript size for TRP-PLIK (Fig. 1B) (*7*). SDS–polyacrylamide gel electrophoresis (SDS-PAGE) and protein immunoblot analysis of transiently expressed TRP-PLIK modified at the COOH-terminus to contain the hemagglutinin (HA) epitope (TRP-PLIK-HA) revealed a signal migrating at ~220 kD, in accord with the predicted molecular mass of TRP-PLIK (212.4 kD; Fig. 1C) (*8*). Consistent with TRP-PLIK being an integral membrane protein, TRP-PLIK-HA transiently expressed in HM1 cells [human embryonic kidney (HEK)–293 cells stably transfected with the muscarinic type 1 receptor] revealed both punctate membrane and cytoplasmic staining (Fig. 1D) (*9*).

TRP-PLIK and PLIK contain a region with similarity to the catalytic domains of MHCK B and eEF-2 kinase. MHCK B and eEF-2 kinase belong to the atypical α-kinase family (*10–12*). A Clustal W alignment of the catalytic regions of the three proteins revealed that TRP-PLIK contains the first and last of the three conserved glycine residues within the "GXGXXG" nucleotide binding motif that is found in many adenosine triphosphate (ATP)–binding proteins. Further sequence analysis of the proposed kinase domain with the program BLOCKS (www.blocks.fhcrc.org) revealed that residues in TRP-PLIK are similar to the "(R/K)(R/K)HHCR motif" (*13*) in FYVE zinc fingers (*14*). One of the cysteines within this motif is conserved among the three kinases. Mutation of a conserved pair of cysteine residues COOH-terminal to the GXGXXG sequence (Cys^{313} and Cys^{317} in rat eEF-2K) completely inactivated eEF-2K (*15*).

We tested whether TRP-PLIK and PLIK could encode functional protein kinases and probed for possible "dominant-negative" mutations for functional studies by constructing recombinant fusion proteins of the kinase domain and two mutant forms attached to the COOH-terminus of GST. ATP-mut is the kinase domain substitution of aspartate exchanged for the final conserved glycine in the putative ATP-binding motif of TRP-PLIK (Gly^{1796}). Zn-mut is the kinase domain substitution of two cysteines (Cys^{1809} and

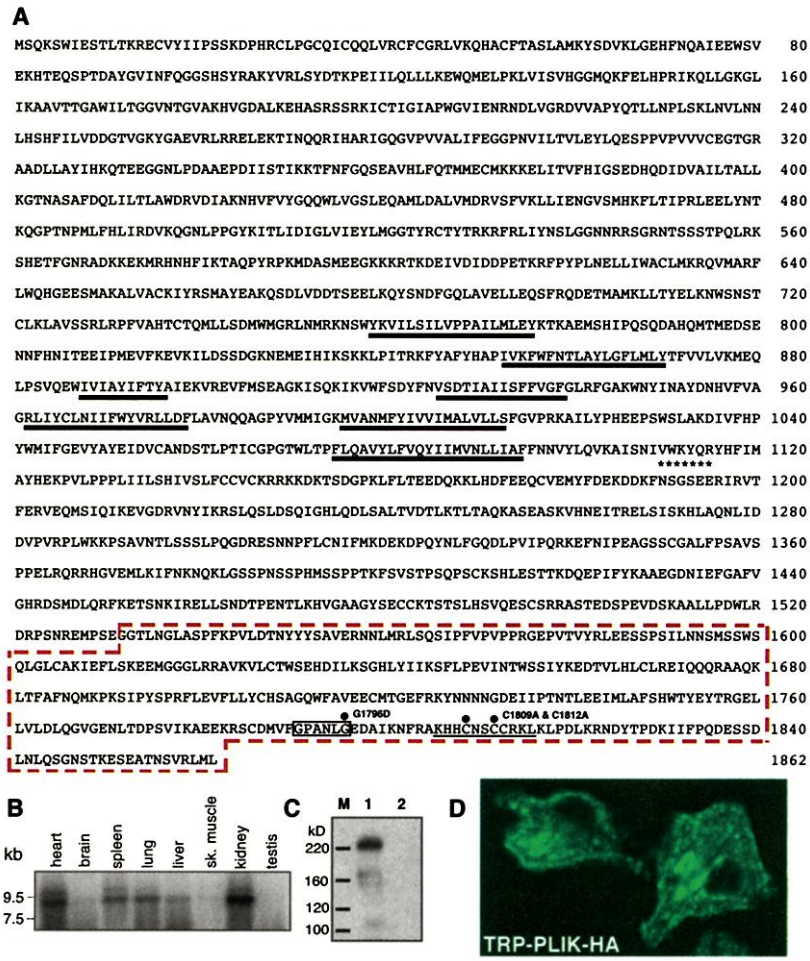

Fig. 1. Sequence of TRP-PLIK and assessment of expression. (**A**) The deduced amino acid sequence of TRP-PLIK (*13*). Secondary structure algorithms and Kyte-Doolittle analysis of the amino acid sequence predict an integral membrane protein with at least six transmembrane domains (underlined). The TRP family amino acid motif "EWKFAR" that follows the last predicted transmembrane domain is modified in TRP-PLIK (VWKYQR) and is underscored by asterisks. The putative kinase domain containing a region homologous to MHCK B and eEF-2 kinase is boxed in red. The "nucleotide binding" motif (GXGXXG) is boxed and the zinc-finger motif is underlined. Residues targeted for mutational analysis are designated by solid black circles. (**B**) Northern blot analysis of TRP-PLIK. (**C**) Expression of full-length TRP-PLIK-HA was assessed by transient transfection of TRP-PLIK-HA (lane 1) or vector (lane 2) into CHO-K1 cells by immunoprecipitation and Western blotting. (**D**) Confocal microscope images of TRP-PLIK-HA expressed in HM1 cells.

Cys[1812]) by alanine within the FYVE zinc finger homology domain from TRP-PLIK (Fig. 1A). GST fusion proteins of the wild-type kinase domain (GST-WT) and kinase domain mutants (GST-ATP-mut and GST-Zn-mut) were expressed in *Escherichia coli* as soluble proteins and purified by glutathione-agarose chromatography. The isolated fusion proteins were used for in vitro kinase assays with myelin basic protein (MBP) as a test substrate (Fig. 2, A and B) (*16*). The incorporation of ^{32}P into MBP catalyzed by GST-WT, but not by GST or MBP alone, indicated that the kinase domain of TRP-PLIK exhibited protein kinase activity. The incorporation of ^{32}P into GST-WT itself is presumably due to autophosphorylation, a common feature of protein kinases (*17*). Indeed, Fig. 2C shows that the full-length TRP-PLIK was autophosphorylated. The incorporation of ^{32}P into MBP catalyzed by GST-ATP-mut was estimated by densitometry to be 0.005 of that for GST-WT, supporting the identification of "GPANLG" (residues 1791 to 1796) (*13*) as the ATP-binding site. No kinase activity by GST-Zn-mut could be detected. Because FYVE zinc fingers are stabilized by interactions of conserved cysteines with Zn^{2+}, the tertiary structure of the enzyme mutant within this region could be destabilized (*18*).

TRP-PLIK was functionally characterized by whole-cell and single-channel recordings of CHO-K1 cells transfected with TRP-PLIK (*19*). In transfected cells, a large outwardly rectifying current was elicited by a voltage ramp and voltage steps ranging from –100 to +100 mV, whereas mock-transfected cells exhibited only a small linear background current (Fig. 3, A and B). Because the large outward current above +50 mV was outside the physiologically relevant range, we focused on the inward currents (see inset in Fig. 3A). Mean inward current density was 15.4 ± 2.6 pA/pF at –100 mV (Fig. 3C).

TRP-PLIK currents were not altered when NaCl was substituted by CH_3SO_3Na, indicating that Cl^- does not permeate TRP-PLIK channels (*6*). The relative permeability of cations

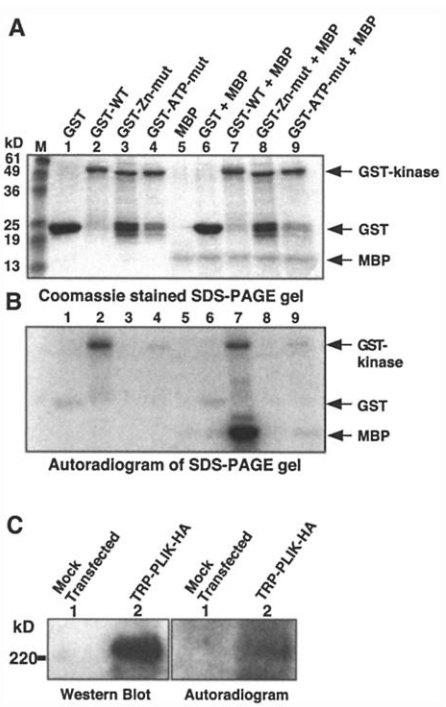

Fig. 2. Kinase activity of TRP-PLIK (*16*). (**A**) Coomassie-stained gel after SDS–gel electrophoresis of phosphorylation reactions containing GST-kinase fusion proteins with or without MBP. lane M, molecular mass marker; lane 1, 10 μg of GST; lane 2, 500 ng of GST-WT; lane 3, 500 ng of GST-Zn-mut; lane 4, 500 ng of GST-ATP-mut; lane 5, 1 μg of MBP; lane 6, GST and 1 μg of MBP; lane 7, GST-WT and 1 μg of MBP; lane 8, GST-Zn-mut and 1 μg of MBP; and lane 9, GST-ATP-mut and 1 μg of MBP. (**B**) Autoradiogram of same sample gel. (**C**) Autophosphorylation of immunoprecipitated HA-tagged TRP-PLIK upon incubation with [γ-^{32}P]ATP.

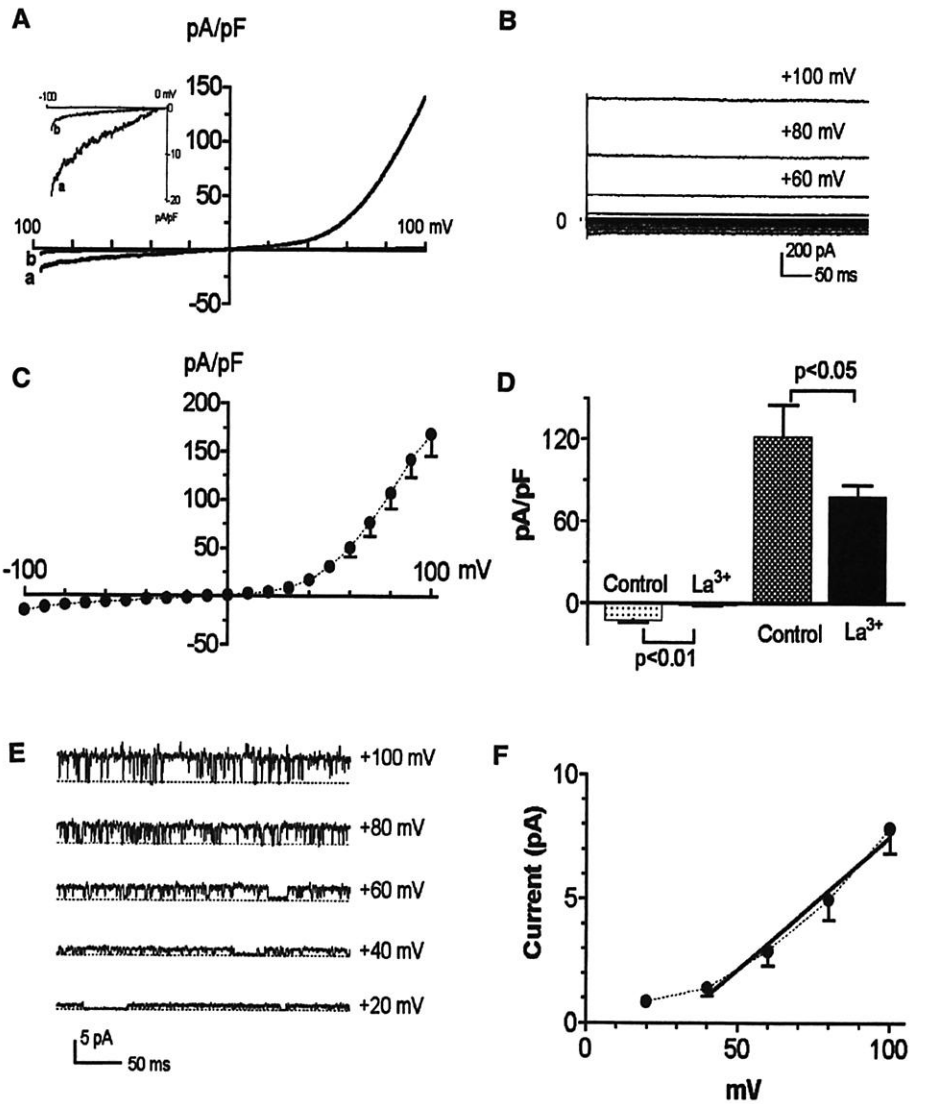

Fig. 3. TRP-PLIK currents in transfected CHO-K1 cells. (**A**) Representative recordings of TRP-PLIK currents evoked by a 500-ms voltage ramp ranging from –100 to +100 mV in TRP-PLIK-transfected (a) and mock-transfected CHO-K1 cells (b). Holding potential = 0 mV. Inset shows current traces obtained during ramps from –100 to 0 mV performed on the same cells but amplified to provide a more detailed view of the inward currents. pA/pF, picoamperes/picofarad. (**B**) Currents elicited by voltage steps ranging from –100 to +100 mV in a TRP-PLIK–expressing cell show that the current steeply rectifies and is time invariant during the duration of the step. (**C**) Averaged *I-V* relation of the TRP-PLIK current (n = 10). (**D**) Blockade of TRP-PLIK by 2 mM La^{3+} (outward currents, upward bars; inward currents, downward bars; ± SEM; n = 5). (**E**) Single-channel currents of TRP-PLIK at various test potentials obtained in outside-out patches. Dashed lines represent the closed state. (**F**) TRP-PLIK single-channel *I-V* relation. Single-channel current amplitude was determined by measuring amplitude histograms at each potential. A linear regression fit from +40 to +100 mV (solid line; ±SEM) yielded a slope conductance of 105 ± 8 pS (n = 4).

relative to that of Cs^+ was 1.1, 0.97, and 0.34 for K^+, Na^+, and Ca^{2+}, respectively. TRP-PLIK was not blocked by 1 mM Ba^{2+}, 1 mM TEA, or 0.2 mM Zn^{2+}. La^{3+} (2 mM) blocked inward and outward TRP-PLIK currents by 97% ($P < 0.01$, $n = 5$) and 37% ($P < 0.05$, $n = 5$), respectively. Single-channel currents were measured at positive voltages in outside-out patches, and their net activity agreed with that predicted from the whole-cell currents. The slope conductance of the single-channel currents was 105 ± 8 pS (Fig. 3, E and F).

We tested the effects of mutations that alter kinase activity on channel function. Whole-cell current amplitudes of ATP-mut and Zn-mut TRP-PLIK were markedly decreased compared with those of the nonmutated TRP-PLIK, suggesting that kinase activity was required for TRP-PLIK channel function (Fig. 4, A and B). This was supported by experiments in which current amplitudes in cells dialyzed with an ATP-containing pipette solution (5 mM ATP, 1 mM Mg^{2+}) initially increased, followed by a slow decrease over several minutes. Currents in cells dialyzed with 0 mM ATP (1 mM Mg^{2+}) pipette solution were significantly smaller and did not vary during recordings (Fig. 4, C and D).

TRP-PLIK is a protein that is both an ion channel and a kinase. As a channel, it conducts calcium and monovalent cations to depolarize cells and increase intracellular calcium. As a kinase, it is capable of phosphorylating TRP-PLIK and other substrates. The kinase activity is necessary for channel function, as shown by its dependence on intracellular ATP and by the kinase mutants. Although kinases have long been known to modulate ion channels (*20*), TRP-PLIK is unusual in that the channel has its own kinase. The presence of the kinase domain adjacent to the sixth transmembrane segment (S6) supports the hypothesis that it plays an important role in channel gating, because S6 appears to be commonly involved in the gating of ion channels (*21*). We postulate that TRP-PLIK is controlled by intracellular ATP levels and may be linked to a signal transduction cascade that modulates the channel's kinase activity. This member of the LTRPC family may link calcium-dependent processes in cells, such as cell division and apoptosis, to receptor and plasma membrane–associated signal transduction events.

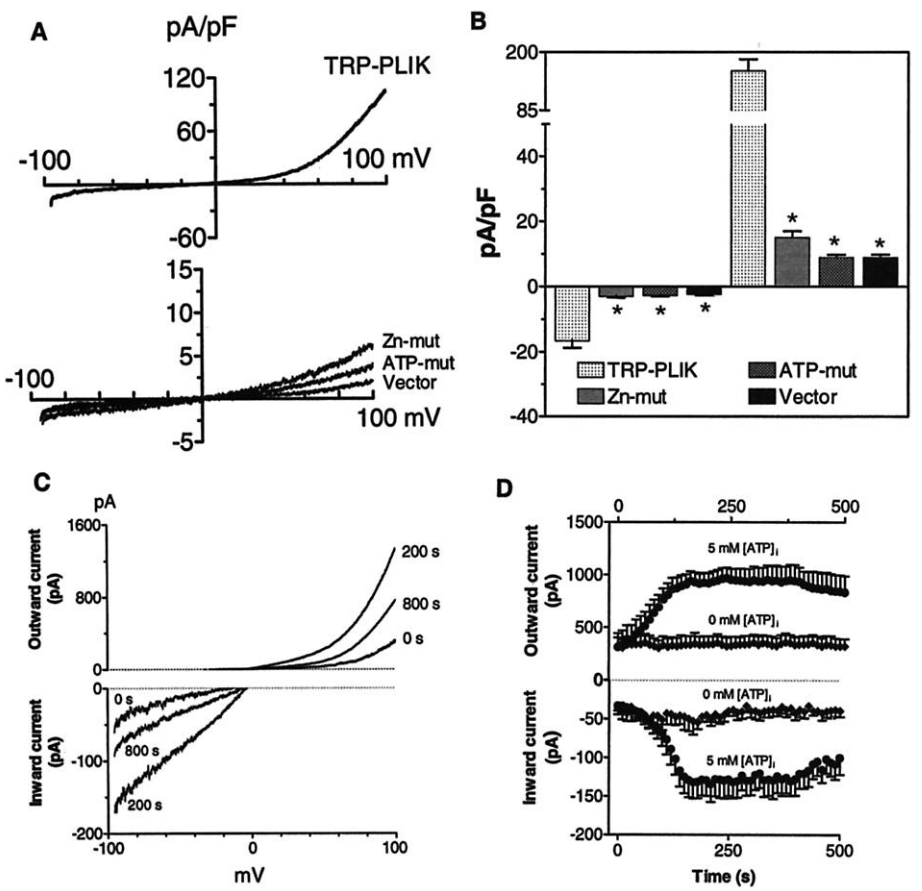

Fig. 4. TRP-PLIK channels are controlled by kinase activity. (**A**) Representative currents recorded in TRP-PLIK–expressing cells (top) and currents elicited by voltage ramps in Zn-mut, ATP-mut, and mock (vector)–transfected CHO-K1 cells (bottom). (**B**) Mean current amplitude (±SEM, $n = 8$) of TRP-PLIK, Zn-mut, ATP-mut, and control (vector). Upward bars, outward current; downward bars, inward current. * indicates $P < 0.01$ compared with TRP-PLIK. (**C**) Representative outward (top) and inward TRP-PLIK currents (bottom) recorded at 0, 200, and 800 s after initiation of whole-cell dialysis. (**D**) Time-dependent changes in TRP-PLIK current amplitude in cells dialyzed with either 0 or 5 mM ATP (1 mM Mg^{2+}) in normal intracellular solution (±SEM, $n = 5$).

References and Notes

1. B. T. Bloomquist *et al.*, *Cell* **54**, 723 (1988).
2. C. Montell, G. M. Rubin, *Neuron* **2**, 1313 (1989).
3. C. Harteneck, T. D. Plant, G. Schultz, *Trends Neurosci.* **23**, 159 (2000).
4. Cloning of PLIK: Sequence shown in supplementary material (*22*). RACE experiments were performed to determine the open reading frame of PLIK and its 5′ untranslated region (UTR) with rat brain Marathon cDNA (Clontech). Description of the primers and conditions for cloning is available upon request.
5. Cloning of mouse TRP-PLIK, TRP-PLIK-HA, TRP-PLIK mutants, and GST-kinase and mutants: TRP-PLIK was cloned directly by PCR with primers based on the deposited sequence of ChaK (nucleotides 95 to 6333) by M. Matsushita (accession number: AF149013). Description of the primers and conditions for cloning is available upon request. TRP-PLIK lacks a CAG codon for alanine at residue 1494 of ChaK, which is most likely due to a polymorphism. To make TRP-PLIK-HA, we first introduced a Cla I site into TRP-PLIK by exchanging the last two codons (ATA GAG to ATC GAT) using the QuikChange site-directed mutagenesis kit (Stratagene). A synthetic oligonucleotide encoding the HA tag (YPYDVPDYA) was then subcloned into the Cla I site. QuikChange was also used to make the ATP-mut substitution (GGA to GAT) and the Zn-mut double substitution (TGT to GCT and TGC to GCC). The "kinase domain" of TRP-PLIK (residues 1532 to 1862) was directionally subcloned in frame with GST into the Bam HI and Eco RI sites of the pGEX-6P-3 vector. GST and GST-fusion proteins were expressed in BL21-CodonPlus(DE3)-RP strain of *E. coli* (Stratagene).
6. L. W. Runnels, L. Yue, D. E. Clapham, data not shown.
7. An adult multiple mouse tissue Northern blot (Clontech) was probed with an RNA probe derived from a 507-bp fragment from the 3′ UTR of ChaK (5827 to 6338). Hybridization of the blot was performed at 68°C in ULTRAhyb (Ambion) for 12 hours, with 1 × 10^6 cpm/ml of probe. Autoradiography was performed for 48 hours with a storage phosphor screen on STORM (Molecular Dynamics).
8. HEK-293 cells or CHO-K1 cells grown on 100-mm dishes were transiently transfected with 8 μg of TRP-PLIK-HA in the pTracer-CMV2 vector with LipofectAMINE 2000. Cells were harvested after 48 hours with 3 ml of RIPA buffer [50 mM tris (pH 7.4), 150 mM NaCl, 1 mM EDTA, 1% IGEPAL CA-630, 0.5% (w/v) deoxycholate, 0.1% (w/v) SDS, and 10 mM iodoacetamide]. TRP-PLIK-HA was immunoprecipitated with mouse monoclonal immunoglobulin G2a (IgG2a) HA probe (F-7) coupled to agarose (Santa Cruz Biotechnology). The agarose was sedimented and washed three times with RIPA buffer, and 2× SDS sample buffer was added. The samples were resolved by SDS-PAGE and Western blotting following standard methods. HA probe Y-11 antibody was the primary antibody (Santa Cruz Biotechnology), and horseradish peroxidase–linked antibody to rabbit Ig (Amersham Pharmacia Biotech) was the secondary antibody. The SuperSignal West Dura substrate was used for chemiluminescent detection (Pierce).
9. HM1 cells grown on glass cover slips were transiently transfected with 1 μg of TRP-PLIK-HA in the pTracer-CMV2 vector with LipofectAMINE 2000 (Life Technologies). Cells were fixed 48 hours after transfection at room temperature for 10 min in phosphate-buffered saline (pH 7.4) with 4% paraformaldehyde (Electron Microscopy Sciences). HA probe Y-11 antibody was the primary antibody, and a 1:2500 dilution of Alexa Fluor 568 goat antibody to rabbit was used for the secondary antibody. Cells expressing green fluorescent protein (GFP) were selected for immunofluorescence imaging.

10. L. M. Futey, Q. G. Medley, G. P. Cote, T. T. Egelhoff, *J. Biol. Chem.* **270**, 523 (1995).
11. A. G. Ryazanov *et al.*, *Proc. Natl. Acad. Sci. U.S.A.* **94**, 4884 (1997).
12. A. G. Ryazanov, K. S. Pavur, M. V. Dorovkov, *Curr. Biol.* **9**, R43 (1999).
13. Single-letter abbreviations for the amino acid residues are as follows: A, Ala; C, Cys; D, Asp; E, Glu; F, Phe; G, Gly; H, His; I, Ile; K, Lys; L, Leu; M, Met; N, Asn; P, Pro; Q, Gln; R, Arg; S, Ser; T, Thr; V, Val; W, Trp; and Y, Tyr.
14. H. Stenmark, R. Aasland, B. H. Toh, A. D'Arrigo, *J. Biol. Chem.* **271**, 24048 (1996).
15. T. A. Diggle, C. K. Seehra, S. Hase, N. T. Redpath, *FEBS Lett.* **457**, 189 (1999).
16. Phosphorylation reactions containing purified GST-kinase fusion proteins and mutants were incubated at 37°C for 30 min in the presence or absence of MBP as a test substrate in a 50-μl reaction. These reactions were performed in KIN buffer {50 mM Mops (pH 7.2), 100 mM NaCl, 20 mM $MgCl_2$, 0.5 mM ATP, and 2 μCi of [γ-^{32}P]ATP}. Immunokinase reactions containing immunopurified TRP-PLIK-HA (*8*) were incubated at 37°C for 30 min in a 50-μl reaction containing KIN buffer with 75 mM *n*-octyl-β-D-glucopyranoside. The reactions were terminated by the addition of 2× SDS sample buffer, and the proteins were resolved by SDS-PAGE and Coomassie staining for the GST-kinase experiment or by SDS-PAGE and Western blotting for the immunokinase assay. The gels were dried, and ^{32}P incorporation was visualized by autoradiography for the GST-kinase experiment. For the immunokinase experiment, ^{32}P incorporation was visualized by autoradiography of the transferred proteins on polyvinylidene difluoride membrane (Bio-Rad) before Western blotting.
17. S. K. Hanks, T. Hunter, *FASEB J.* **9**, 576 (1995).
18. S. Misra, J. H. Hurley, *Cell* **97**, 657 (1999).
19. The TRP-PLIK clone in the pTracerCMV2 (Invitrogen) vector was transiently transfected with LipofectAMINE 2000 (Gibco). Cells were transferred to cover slips 12 hours after transfection, and electrophysiological measurements were made 24 hours after transfection (22 ± 2°C). The TRP-PLIK–expressing CHO-K1 cells were detected by GFP fluorescence. Membrane currents were digitized at 10 or 20 kHz and digitally filtered off line at 1 kHz. Voltage stimuli lasting 500 ms were delivered at 5-s intervals, with either voltage ramps or voltage steps from −100 to +100 mV. The internal pipette solution for macroscopic and single-channel currents contained 145 mM Cs-methanesulfonate, 8 mM NaCl, 5 mM ATP, 1 mM $MgCl_2$, 10 mM EGTA, 4.1 mM $CaCl_2$, and 10 mM Hepes, with pH adjusted to 7.2 with CsOH after addition of ATP. The standard extracellular solution contained 140 mM NaCl, 5 mM CsCl, 2.8 mM KCl, 2 mM $CaCl_2$, 1 mM $MgCl_2$, 10 mM Hepes, and 10 mM glucose, with pH adjusted to 7.4 with NaOH. Relative ion permeabilities were measured with the pipette solution containing 145 mM Cs-methanesulfonate, 10 mM CsCl, 5 mM ATP, 10 mM EGTA, and 10 mM Hepes (pH 7.2) and the external solution containing 110 mM $NMDG^+$, 30 mM X^+ (Na^+, Ca^{2+}, K^+, or Cs^+), 10 mM Hepes, and 10 mM glucose (pH 7.4). The relative permeability for monovalent ions was calculated according to the equation $P_X/P_{Cs} = ([Cs^+]_o/[X^+]_o)\exp[F(E_X - E_{Cs})/RT]$. The P_{Ca}/P_{Cs} permeability ratio was calculated according to the equation $P_{Ca}/P_{Cs} = \{[Cs^+]_o\exp(-FE_{Cs}/RT)\exp(FE_{Ca}/RT)[\exp(FE_{Ca}/RT)+1]\}/(4[Ca^{2+}]_o)$, where *R*, *T*, and *F* are the gas constant, absolute temperature, and Faraday's constant, respectively. Statistical comparisons were made with the two-way analysis of variance (ANOVA) and two-tailed *t* test with Bonferroni correction; $P < 0.05$ indicated statistical significance.
20. I. B. Levitan, *Adv. Second Messenger Phosphoprotein Res.* **33**, 3(1999).
21. G. Yellen, *Q. Rev. Biophys.* **31**, 239 (1998).
22. Supplementary data are available at www.sciencemag.org/cgi/content/full/1058519/DC1.

21 December 2000; accepted 9 January 2001
Published online 18 January 2001;
10.1126/science.1058519
Include this information when citing this paper.

Role of the ENTH Domain in Phosphatidylinositol-4,5-Bisphosphate Binding and Endocytosis

Toshiki Itoh,[1] Seizo Koshiba,[2] Takanori Kigawa,[2,3] Akira Kikuchi,[4] Shigeyuki Yokoyama,[2,3,5] Tadaomi Takenawa[1]*

Endocytic proteins such as epsin, AP180, and Hip1R (Sla2p) share a conserved modular region termed the epsin NH_2-terminal homology (ENTH) domain, which plays a crucial role in clathrin-mediated endocytosis through an unknown target. Here, we demonstrate a strong affinity of the ENTH domain for phosphatidylinositol-4,5-bisphosphate [PtdIns(4,5)P_2]. With nuclear magnetic resonance analysis of the epsin ENTH domain, we determined that a cleft formed with positively charged residues contributed to phosphoinositide binding. Overexpression of a mutant, epsin Lys^{76} → Ala^{76}, with an ENTH domain defective in phosphoinositide binding, blocked epidermal growth factor internalization in COS-7 cells. Thus, interaction between the ENTH domain and PtdIns(4,5)P_2 is essential for endocytosis mediated by clathrin-coated pits.

ENTH domains are structural modules of ~140 amino acids found in mammalian epsin 1 and 2, AP180, and Hip1R, as well as in their yeast homologs, Ent1p through Ent4p, yAP180, and Sla2p (*1–4*). Mammalian epsin plays a crucial role in clathrin-mediated endocytosis (*2*). Yeast Ent1p and Ent2p are essential for actin function and for endocytosis. Disruption of both genes in yeast is lethal, and the ENTH domain is required to inhibit lethality. Almost all temperature-sensitive alleles of the ENT1 gene are found within the ENTH domain, supporting its importance (*3*). The essential function of the conserved ENTH domain from yeast to mammal prompted us to identify its downstream target. Using an ENTH affinity chromatography column, we were not able to detect any protein from bovine brain extract bound to the epsin ENTH domain. Because clathrin-mediated endocytosis is mediated by a specific interaction between endocytic proteins and the lipid bilayer to form invaginated buds and coated vesicles (*5*, *6*), and because many biochemical and physiological studies suggest important roles for phosphoinositides in endocytosis and vesicular trafficking (*7–9*), we examined the possibility that the ENTH domain binds to phosphoinositides.

To determine whether the ENTH domain could bind phosphoinositides, we subjected a glutathione *S*-transferase (GST) fusion protein of the epsin ENTH domain to liposome binding assay. Although epsin ENTH did not co-sediment with phosphatidylethanolamine (PE)– and phosphatidylcholine (PC)–based liposomes, increasing concentrations of phosphatidylinositol4,5-bisphosphate [PtdIns(4,5)P_2] in the liposomes resulted in co-sedimentation of the ENTH domain (Fig. 1A). Co-sedimentation was not observed in the presence of increased concentrations of PtdIns in the liposomes, demonstrating a high specificity for the interaction with PtdIns(4,5)P_2. Co-sedimentation was clearly observed at 0.2% PtdIns(4,5)P_2, and the dissociation constant K_d for the interaction was estimated at 0.37 μM. The strong interaction between the ENTH domain and PtdIns(4,5)P_2 was confirmed by other methods, including overlay assays with protein probe against phospholipids (Fig. 1B) and lipid probe against the ENTH domain blotted onto nitrocellulose membrane (Fig. 1C). The specificity of the binding was then studied with all known mammalian phosphoinositides. PtdIns(3,4,5)P_3 also showed substantial binding, whereas PtdIns, PtdIns3P, PtdIns4P, PtdIns5P, PtdIns(3,4)P_2, and PtdIns(3,5)P_2 exhibited far lower affinities (Fig. 1D). No binding was observed of other acidic phospholipids, such as phosphatidic acid and phosphatidylserine (Fig. 1D). We also carried out liposome binding assays for the AP180 ENTH domain. AP180 ENTH bound to PtdIns(4,5)P_2 strongly and also showed a lower affinity for PtdIns(3,4,5)P_3 (Fig. 1E).

[1]Department of Biochemistry, Institute of Medical Science, University of Tokyo, 4-6-1 Shirokanedai, Minato-ku, Tokyo 108-8639, Japan. [2]RIKEN Genomic Sciences Center, 1-7-22 Suehiro-cho, Tsurumi-ku, Yokohama-shi, Kanagawa 230-0045, Japan. [3]Cellular Signaling Laboratory, RIKEN Harima Institute at SPring-8, 1-1-1 Kouto, Mikazuki-cho, Sayo, Hyogo 679-5148, Japan. [4]Department of Biochemistry, Hiroshima University School of Medicine, 1-2-3 Kasumi, Minami-ku, Hiroshima 734–8551, Japan. [5]Department of Biophysics and Biochemistry, Graduate School of Science, University of Tokyo, 7-3-1 Hongo, Bunkyo-ku, Tokyo 113-0033, Japan.

*To whom correspondence should be addressed. E-mail: takenawa@ims.u-tokyo.ac.jp